



**HAL**  
open science

## **Impact of phenolic composition and antioxidant parameters on the ageing potential of Syrah red wines measured by accelerated ageing tests**

Luca Garcia, Stacy Deshaies, Thibaut Constantin, François Garcia, Cédric Saucier

### ► **To cite this version:**

Luca Garcia, Stacy Deshaies, Thibaut Constantin, François Garcia, Cédric Saucier. Impact of phenolic composition and antioxidant parameters on the ageing potential of Syrah red wines measured by accelerated ageing tests. *Food Chemistry*, 2023, 426, pp.136613. <10.1016/j.foodchem.2023.136613>. <hal-04369728>

**HAL Id: hal-04369728**

**<https://hal.inrae.fr/hal-04369728v1>**

Submitted on 9 Jul 2025

**HAL** is a multi-disciplinary open access archive for the deposit and dissemination of scientific research documents, whether they are published or not. The documents may come from teaching and research institutions in France or abroad, or from public or private research centers.

L'archive ouverte pluridisciplinaire **HAL**, est destinée au dépôt et à la diffusion de documents scientifiques de niveau recherche, publiés ou non, émanant des établissements d'enseignement et de recherche français ou étrangers, des laboratoires publics ou privés.



Copyright - All rights reserved

1     **Impact of phenolic composition and antioxidant parameters on the ageing**  
2             **potential of Syrah red wines measured by accelerated ageing tests**

3  
4     Luca Garcia<sup>a</sup>, Stacy Deshaies<sup>a</sup>, Thibaut Constantin<sup>a</sup>, François Garcia<sup>a</sup> and Cédric Saucier<sup>a</sup>.

5     a - SPO, Univ Montpellier, INRAE, Institut Agro, Montpellier, France

6     \* Corresponding author: Tel.: +33411759567; Fax: +33411759638. E-mail address:  
7     cedric.saucier@umontpellier.fr (Saucier, C.).

8     **Abstract**

9     Fourteen Syrah red wines with different initial composition and antioxidant properties  
10     (polyphenols, antioxidant capacity, voltammetric behaviour, colour parameters and SO<sub>2</sub>) were  
11     selected. Three different accelerated ageing tests (AATs) were then performed on these wine:  
12     thermal test at 60°C (60°C-ATT), enzymatic test with laccase (Laccase-ATT) and chemical  
13     test with H<sub>2</sub>O<sub>2</sub> (H<sub>2</sub>O<sub>2</sub>-ATT). The results showed high correlations between the initial phenolic  
14     composition and antioxidant properties of the samples. Partial least squares (PLS) regressions  
15     were used in order to establish some models that can predict the AATs test results based on  
16     their different initial composition and antioxidant properties. The PLS regression models had  
17     overall very good accuracy and involved different explaining variables for each test. The  
18     models taking into account all the measured parameters and the phenolic composition alone  
19     showed good predictive capacities with correlation coefficients ( $r^2$ ) > 0.89.

20  
21     **Keywords:**

22     Wine

23 Syrah

24 Oxidation

25 Polyphenols

26 Ageing

27 Antioxidant

## 28 **1. Introduction**

29 Wine ageing is an important step in the elaboration of high-quality wines, especially for red  
30 wines. The process is divided into two key steps. The first one is the maturation phase (bulk  
31 storage in barrel or tank) and the second one is the ageing phase after bottling (A. Waterhouse  
32 et al., 2016). During wine ageing, many reactions take place, which will modify and improve  
33 the organoleptic parameters of the wine over time (Tao et al., 2014).

34 Oxygen is one of the most important parameters in all these reactions throughout the wine  
35 making process, especially during the maturation phase. Indeed, it is known that the good  
36 quality of a red wine is associated with a moderate and controlled exposure to oxygen  
37 throughout the winemaking and ageing process (Ugliano, 2013). The addition of oxygen is  
38 generally necessary during the maturation of red wines. This occurs during different stages of  
39 the winemaking process or micro-oxygenation during barrel ageing (exchange through the  
40 barrel) or during bottle ageing through the cork. It is particularly important for the  
41 improvement of red wine quality and will stabilise the colour and improve the mouthfeel  
42 (Kilmartin, 2009).

43 From an organoleptic point of view the bouquet of the wine changes radically during wine  
44 ageing. This change is the result of a complex set of chemical reactions and in most cases,  
45 oxygen contributes to these reactions. There are two different possible general chemical

46 pathways: the oxidation of aroma compounds and also the formation of new aroma  
47 compounds by oxidation. In particular the formation of oxidative aromas such as acetaldehyde  
48 or sotolon, and the formation/degradation of volatile sulphur compounds such as hydrogen  
49 sulfide or methanethiol (Ferreira et al., 2014; Ugliano, 2013).

50 In addition to the evolution of aromas, the colour of red wine also changes during red wine  
51 ageing. These changes are due to the evolution of the native anthocyanins extracted during the  
52 maceration of grapes. Their content decreases over time (Alcalde-Eon et al., 2006), as they  
53 react with other constituents of the wine such as flavanols (Salas et al., 2004) or with yeast  
54 metabolites such as acetaldehyde or pyruvic acid or glyoxal to form new pigments (Fulcrand  
55 et al., 1998). The new anthocyanins formed possess more stable structures and lead to  
56 stabilisation of wine colour (Echave et al., 2021), as well as bathochromic and hypsochromic  
57 changes (Brouillard et al., 1997). In addition, condensation between flavan-3-ols and  
58 anthocyanins by yeast derivatives can yield to the formation of yellow-orange xanthylum  
59 derivatives (A. Waterhouse et al., 2016). The formation of all these new pigments during  
60 ageing is responsible of the observed changes in wine colour, i.e. from red-purple hue to a  
61 brick-red hue (Ribéreau-Gayon & Peynaud, 1966).

62 Concerning mouthfeel properties, a decrease in astringency and bitterness is also observed  
63 during red wine ageing. This is due to oxidative and non-oxidative polymerisations and  
64 precipitation of phenolic compounds such as tannins especially during storage in the bottle  
65 (Echave et al., 2021).

66 All these evolutions can take place quickly depending on the wine studied and influence the  
67 wine ageing capacity. This capacity is also linked to the different terroirs and grape variety  
68 used, the winemaking process and the stopper used during bottle ageing. In general, high  
69 quality red wines require a period of bottle ageing to reach an optimum before consumption  
70 (Gambutì et al., 2013). The ageing capacity is then related to the capacity of a wine to

71 undergo oxidation over time (A. L. Waterhouse & Miao, 2021). It is therefore necessary to  
72 understand how the wine evolves during an exposure to oxygen.

73 When oxygen is dissolved in wine, it can rapidly react with many wine components,  
74 especially with phenolic compounds which are one of the main substrates for oxidation  
75 (Oliveira et al., 2011). Although individual phenols may react very differently to oxygen, the  
76 total phenol composition of a wine can give an estimate of its ability to react with oxygen  
77 (Singleton, 1987) and then to resist to oxidation. As shown by Ferreira et al (Ferreira et al.,  
78 2015) the average oxygen consumption rate is related to the total polyphenols measured by  
79 the Folin-Ciocalteu method. Phenolic compounds with ortho-catechol groups (anthocyanins,  
80 proanthocyanidins and flavan-3-ols) can form highly reactive species such as quinones,  
81 radicals and hydrogen peroxide due to the catalytic action of metals such as copper and iron  
82 (Kilmartin, 2009; A. L. Waterhouse & Laurie, 2006). These species may induce the oxidation  
83 of various other wine components in particular, SO<sub>2</sub>, phenolics, carbonyls and thiols (Ferreira  
84 et al., 2015; Ugliano, 2013).

85 Previous studies have shown that higher pH (Singleton, 1987) and addition of ellagitannins  
86 can increase oxygen consumption rate (Vivas & Glories, 1996). Furthermore, oxygen  
87 consumption rate is positively correlated with concentrations of metals such as copper,  
88 tannins rich in epigallocatechin and epicatechin-3-O-gallate (Carrascón et al., 2018; Ferreira  
89 et al., 2015).

90 Accelerated ageing tests (AATs) were recently developed in our laboratory (Deshaies 2020)  
91 in order to accelerate the oxidation process for red wines. These tests consist of monitoring  
92 oxygen consumption of red wines in the presence of hydrogen peroxide (H<sub>2</sub>O<sub>2</sub>-ATT) or  
93 laccase (laccase-ATT) oxidising agent or a temperature increase at 60°C (60°-ATT).  
94 Moreover, as these ageing tests use different physico-chemical conditions, they will target

95 different chemical pathways and may also depend on the type of wine and on its initial  
96 composition.

97 The objectives of this article are:

- 98 • To obtain chemical characterization of Syrah red wine samples.
- 99 • To obtain the antioxidant capacity (radical scavenging capacity and ferric reducing  
100 capacity) of these wines.
- 101 • To determine the cyclic voltammetry behaviour of these wines.
- 102 • To build PLS regression models based on wine composition and antioxidant  
103 capacity to predict AATs results for these wines.

## 104 **2. Material and methods**

### 105 **2.1. Reagents, solvents, and standards**

106 Hydrogen peroxide solution 30% (ACS reagent) and Folin-Ciocalteu reagent were  
107 obtained from Carlo Erba Reagents (Peypin, France). Laccase from *Trametes versicolor* (0.78  
108 U/mg), gallic acid, phloroglucinol, catechin, Trolox, 2,2'-azino-bis (3-ethylbenzothiazoline-6-  
109 sulfonic acid) diammonium salt (ABTS), potassium persulfate, sodium hydrogen sulfite  
110 (NaHSO<sub>3</sub>) and hydrochloric acid (37%) were obtained from Sigma-Aldrich (Saint-Quentin  
111 Fallavier, France). Ferric chloride, 2,4,6-tri(2-pyridyl)-s-triazine (TPTZ) and ferrous sulfate  
112 heptahydrate were purchased from Alfa Aesar (Kandel, Germany). Oenin Chloride was  
113 obtained from Extrasynthese (Genay, France).

### 114 **2.2. Wines samples**

115 Fourteen red wines samples (100% Syrah) from the same vintage (2019) were obtained  
116 in different wineries from Côtes du Rhône and Languedoc-Roussillon area (Table 1).

---

Code	Grape variety	Denomination of origin	Vintage	Ageing
------	---------------	------------------------	---------	--------

---

LR12-B19	Syrah	Languedoc-Roussillon	2019	Oak barrel	117	<i>Table</i>
LR7-C19	Syrah	Languedoc-Roussillon	2019	Tank		
LR10-B19	Syrah	Languedoc-Roussillon	2019	Oak barrel	118	<i>l.</i>
LR1-C19	Syrah	Languedoc-Roussillon	2019	Tank		
LR8-B19-1	Syrah	Languedoc-Roussillon	2019	Oak barrel	119	<i>Charact</i>
LR8-B19-2	Syrah	Languedoc-Roussillon	2019	Oak barrel		
LR9-B19-1	Syrah	Languedoc-Roussillon	2019	Oak barrel	120	<i>eristics</i>
LR9-B19-2	Syrah	Languedoc-Roussillon	2019	Oak barrel	121	<i>of the</i>
LR6-B19	Syrah	Languedoc-Roussillon	2019	Oak barrel		
LR4-B19	Syrah	Languedoc-Roussillon	2019	Oak barrel	122	<i>red</i>
LR2-B19	Syrah	Languedoc-Roussillon	2019	Oak barrel		
CR1-C19	Syrah	Côtes du Rhône	2019	Tank	123	<i>wines</i>
CR12-B19-1	Syrah	Côtes du Rhône	2019	Oak barrel		
CR12-B19-2	Syrah	Côtes du Rhône	2019	Oak barrel	124	<i>samples</i>

125

126

127

128

129

130

131

132

133

134

135 Three 750 mL bottles of each wine were opened and slowly homogenized under nitrogen and  
 136 aliquots of 50 mL tubes were then immediately frozen at -80 °C.

### 137 **2.3. Accelerated ageing tests (ATTs)**

138 Three accelerated ageing tests were applied to wine samples as described by Deshaies  
 139 et al. (Deshaies et al., 2020). Each wine sample was saturated with air by vigorously shaking a  
 140 500 mL flask containing 50 mL of wine for 10 s, after which the cap was opened (5 s) to let  
 141 fresh air enter the flask. This saturation operation was repeated three times. Then, 11 mL of  
 142 saturated red wine was added into a Hermetic Pyrex 11 mL cultures tubes (VWR 734-4224,  
 143 Radnor, PA, USA) containing Pst3 oxygen sensors (Presens-Precision Sensing GmbH,

144 Regensburg, Germany). For the Laccase-ATT 50  $\mu\text{L}$  of a  $10 \text{ g}\cdot\text{L}^{-1}$  laccase from *Trametes*  
145 *versicolor* solution was added. For  $\text{H}_2\text{O}_2$ -ATT, 20  $\mu\text{L}$  of hydrogen peroxide solution (30%)  
146 was added. Finally, the thermal treatment was performed by heating the 11 mL of wine at 60  
147  $^\circ\text{C}$ . The dissolved oxygen rate concentration was followed during the tests by  
148 oxoluminescence. Assuming first order kinetic, oxygen consumption rate constants (k) for  
149 each AATs were calculated.

## 150 **2.4.Total polyphenols and anthocyanins analysis**

### 151 **2.4.1. Total Polyphenols Content (TPC) determination**

152 The determination of the total phenolics compounds content in red wine was  
153 determined by the Folin–Ciocalteu method and performed on a microplate reader (BMG  
154 Labtech, Germany) using spectrophotometric detection and microliter 96-well plates,  
155 according to the method described in Deshaies et al. (Deshaies et al., 2021). Briefly, fifty  
156 microliters of diluted wine (1:100, v/v) or standard were mixed with 50  $\mu\text{L}$  of Folin–Ciocalteu  
157 reagent (1:5, v/v) and 100  $\mu\text{L}$  of sodium hydroxide solution ( $0.35 \text{ mol}\cdot\text{L}^{-1}$ ) in each well.  
158 After a period of 3 min of incubation, the absorbance of each sample was monitored at 750  
159 nm. A standard curve of gallic acid ( $0 - 200 \text{ mg}\cdot\text{L}^{-1}$ ) was prepared and the results were  
160 expressed as  $\text{g}\cdot\text{L}^{-1}$  of gallic acid equivalents (GAE).

### 161 **2.4.2. Total Polyphenols Index (TPI) determination**

162 Total Polyphenols Index (TPI) were determined by UV–visible spectrophotometry  
163 (Agilent Carry 60 spectrometer, Agilent) at 280 nm with 1 cm cells after dilution in water  
164 (1:100 v/v) (Ribéreau-Gayon, 1970).

### 165 **2.4.3. Total Anthocyanins (TA) determination**

166 Total Anthocyanins contents were determined as described by Ribéreau-Gayon and  
167 Stonestreet (Ribéreau-Gayon & Stonestreet, 1965). One mL of wine samples, 1 mL of ethanol  
168 0,1% HCl and 20mL of  $\text{H}_2\text{O}$  2% HCl were mixed. Then 10 mL of this solution were placed in

169 two test tubes. In one of them was added 4 mL of water (1) and in the other one 4 mL of a  
170 15% solution of NaHSO<sub>3</sub> (2). After 15 min, absorbance at 520 nm of each tube was measured  
171 (Agilent Carry 60 spectrometer, Agilent, Les Ulis, France). The concentration of total  
172 anthocyanins (TA) in mg.L<sup>-1</sup> was calculated by the following equation :

$$173 \quad \text{TA (mg.L}^{-1}\text{)} = 875 \times (\text{A1} - \text{A2})$$

## 174 **2.5. Antioxidant capacity measurements**

### 175 **2.5.1. Determination of radical scavenging activity using ABTS (TEAC** 176 **assay)**

177 ABTS antioxidant capacity was performed on a microplate reader (BMG Labtech,  
178 Germany) using spectrophotometric detection and microliter 96-well plates, according to  
179 Muller et al. (Muller et al., 2010) with slight modifications. To generate ABTS radicals, 5mL  
180 of ABTS solution (7 mM) was added to 5 mL of a potassium persulfate solution (2.45 mM)  
181 prepared in sodium acetate buffer (50 mM, pH = 4,6). The mixture was incubated at room  
182 temperature in the dark all night. The stock solution was diluted with acetate buffer to an  
183 absorbance of  $0.7 \pm 0.02$  at 734 nm. Twenty microliters of diluted red wine (1:100, v/v) or  
184 standard were mixed with 200  $\mu\text{L}$  of ABTS solution. After 7 min, the absorbance was  
185 measured at 734 nm. A standard curve of Trolox (0 - 250  $\mu\text{mol.L}^{-1}$ ) was used. Results (Trolox  
186 Equivalent Antioxidant Capacity) were expressed as  $\text{mmol.L}^{-1}$  Trolox Equivalent (TE).

### 187 **2.5.2. Ferric-Reducing Antioxidant Power (FRAP assay)**

188 FRAP antioxidant capacity determination was performed on a microplate reader  
189 (BMG Labtech, Germany) using spectrophotometric detection and microliter 96-well plates,  
190 according to Sulleria et al. (Suleria et al., 2020) with slight modifications. To prepare the  
191 FRAP reagent, 300 mM sodium acetate buffer (pH 3.6), 10 mM TPTZ solution in 40 mM  
192 HCl and 20 mM ferric chloride were mixed in a ratio of 10:1:1 (v/v/v). Then, 20  $\mu\text{L}$  of diluted

193 wine samples (1/ 100; v/v) and 280  $\mu\text{L}$  FRAP reagent were mixed in a 96 well plate followed  
194 by incubation at 37 °C for 5 min, and absorbance was measured at 593 nm. A standard curve  
195 of ferrous sulfate heptahydrate (0 - 100  $\mu\text{mol.L}^{-1}$ ) was used. Results were expressed as  
196  $\text{mmol.L}^{-1} \text{Fe}^{2+}$  equivalent.

### 197 **2.5.3. Electrochemical measurements**

198 Cyclic voltammetry measurements were performed as described in Deshaies et al.  
199 (Deshaies et al., 2021). Wine samples were diluted (1:75 v/v) in model wine (ethanol 12%  
200 (v/v), 33  $\text{mmol.L}^{-1}$  tartaric acid and pH 3.6 adjusted with 1  $\text{mol.L}^{-1}$  NaOH) and then 200  $\mu\text{L}$   
201 of diluted sample were dropped on the electrode surface. The measurements were performed  
202 in the range of -0.2 V to 0.8 V (vs.  $\text{Ag}_{(\text{s})}$ ) with a scan rate of 100  $\text{mV.s}^{-1}$  using 4 mm diameter  
203 single-walled carbon nanotubes-modified screen-printed carbon electrode SWCNTs-SPCE  
204 (Dropsens, Oviedo, Spain) in a three-electrode configuration (carbon counter electrode and  
205 silver reference electrode). The experiments were performed on a potentiostat/galvanostat  
206 (Autolab PGSTAT 302N) using software Nova 2.1.5 (Metrohm, Herisau, Switzerland).

207 Different charges corresponding to antioxidant capacities can be extracted from  
208 voltammograms (area under the anodic curve until the chosen potential) (Deshaies et al.,  
209 2021). The total charge  $Q_{800\text{mV}}$  corresponds to all oxidizable phenolic compounds of the wine.  
210  $Q_{240\text{mV}}$  can be assigned to the most oxidizable polyphenols with the highest reducing capacity.  
211  $Q_{520\text{mV}}$  corresponds to all the compounds which oxidize until this potential and the difference  
212  $Q_{520\text{mV}} - Q_{240\text{mV}}$  can be afterwards calculated. Finally,  $Q_{240\text{mV}}/Q_{800\text{mV}}$  ratio indicates the  
213 contribution of the most antioxidant compounds to the total antioxidant capacity of wines.

### 214 **2.6. Free sulfur dioxide determination**

215 Free sulfur dioxide content was determined by aeration/oxidation according to  
216 reference method O.I.V–MA–AS323–04A described in the “Compendium of International

217 Methods of Analysis” published in 2009 by the International Organisation of Vine and Wine  
218 (OIV).

## 219 **2.7.Spectrophotometric colorimetric measurements**

220 Total color intensity (sum of absorbance values at 420, 520 and 620 nm) and hue (ratio  
221 between  $A_{420}$  and  $A_{520}$ ) were determined by UV-visible spectrophotometry (Agilent Carry 60  
222 spectrometer, Agilent, Les Ulis, France) according to reference method OIV-MA-AS2-07B  
223 described in the “Compendium of International Methods of Analysis” published in 2009 by  
224 the International Organisation of Vine and Wine (OIV).

225

## 226 **2.8.Determination of phenolic composition**

### 227 **2.8.1. UHPLC-DAD-MS analysis of monomeric anthocyanins**

228 The quantification of monomeric anthocyanins was performed as described by  
229 Benbougerra et al. (Benbougerra et al., 2020) with slight modifications. After a filtration  
230 on a 0.45  $\mu\text{m}$  PTFE filter (Macherey-Nagel, Düren, Germany), the wines were directly  
231 injected (7.5  $\mu\text{L}$ ) on a UPLC system Waters Acquity (Saint-Quentin-en-Yvelines, France)  
232 equipped with a reversed phase UPLC Acquity UPLC BEH C18 column (50 mm length, 2.1  
233 mm internal diameter, 1.7  $\mu\text{m}$  particle size) from Waters. The method used was a binary  
234 gradient with mobile phase A (0,1% v/v aqueous trifluoroacetic acid) and mobile phase B  
235 (acetonitrile). The column temperature was set at 50 °C. The 40 min elution method at flow  
236 0.25 mL.min<sup>-1</sup> was 1% B (0 min), 1 - 8.8% (0-5 min) B, 8,8 - 20.6% (5-30 min) B, 20.6 - 96%  
237 (30-30.5 min) B, isocratic with 96% B (30.5 - 34 min), 96-1% (34 -34.1 min) B, and isocratic  
238 with 1% B (34.1 - 40 min). The detection was monitored at 520 nm with a photodiode array  
239 detector (PDA). External malvidin-3-O-glucoside calibration curve was used. Results were  
240 expressed as mg malvidin-3-O-glucoside equivalent (M3G eq).L<sup>-1</sup>.

### 241 **2.8.2. UHPLC-DAD-MS analysis of flavanols**

242 The composition of flavanols was studied after acid-catalyzed depolymerization in the  
243 presence of a phloroglucinol as described by Carrascón et al. (Carrascón et al., 2018) with  
244 slight modifications. 400  $\mu\text{L}$  of red wine sample were brought to dryness in a centrifugal  
245 solvent evaporator (Genevac, Ipswich, UK). The obtained residue was dissolved in 600  $\mu\text{L}$  of  
246 a 50  $\text{g}\cdot\text{L}^{-1}$  of phloroglucinol and 10  $\text{g}\cdot\text{L}^{-1}$  of ascorbic acid in methanol-HCl 0.2 M solution. The  
247 reaction was carried out at 50 °C for 20 min, then 600  $\mu\text{L}$  of ammonium acetate 200 mM  
248 solution were added to stop the reaction. Then, the sample was centrifuged at 12,000 rpm for  
249 10 min and the supernatant was injected in the same chromatographic apparatus as mentioned  
250 in section 2.8.1. The method used was a binary gradient with mobile phase A (0.1% v/v  
251 aqueous trifluoroacetic acid) and mobile phase B (acetonitrile). The elution method at flow  
252 0.45  $\text{mL}\cdot\text{min}^{-1}$  was 2% B (0 min), 2-6% B (0-10 min), 6-20% B (10-16 min), 20-99% B (16-  
253 16.1 min), isocratic with 99% B (16.1-18 min), 99-2% B (18-18.1 min) and isocratic with 2%  
254 B (18.1-22 min). The column temperature was 40 °C. Eluting peaks were monitored at 280  
255 nm. This analysis allowed us to obtain the type and the relative proportions of the terminal  
256 and extension units of tannins. The molar ratio between total and terminal units gives access  
257 to the mean degree of polymerization (mDP). External catechin calibration curve was used  
258 and quantification was effected in equivalents of catechin. Concentration of epicatechin,  
259 epigallocatechin and epicatechin-3-O-gallate were estimated using their response factors  
260 relative to catechin.

## 261 **2.9. Statistical Analysis**

262 The ANOVA, correlation, PCA (Principal Component Analysis) and PLS (Partial least-  
263 squares) regression tests were performed using XLSTAT software (Addinsoft version 19.02,  
264 Paris, France). Tukey test was carried out and when p-values were < 0.05 the data were  
265 considered as significant. Pearson's correlation coefficient was carried out for the  
266 determination of correlations. PLS regression models were initially built with all the variables

267 studied and were further simplified by iterative elimination of variables with smaller  
268 contribution to the model. The optimum model was considered to be the one providing the  
269 highest coefficient of determination with the smallest number of variables. All analyses,  
270 experiments and tests were performed in triplicate.

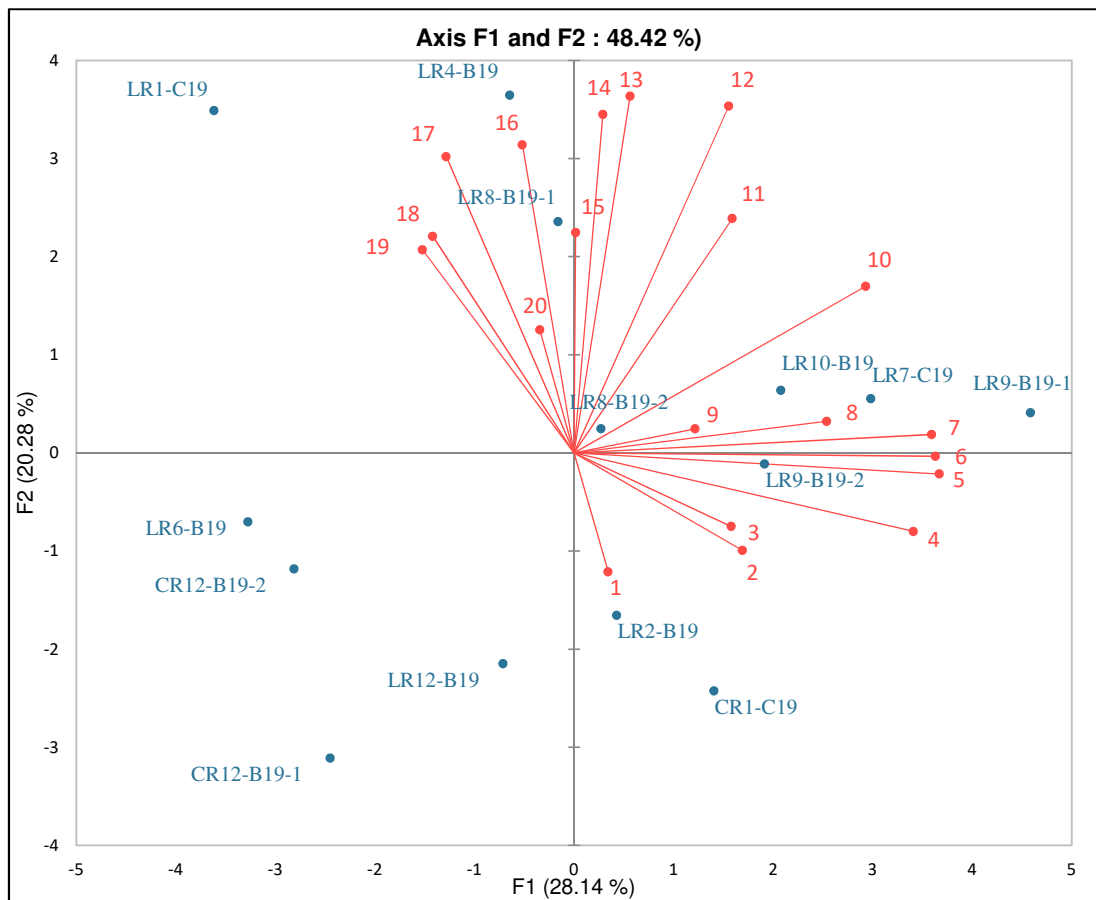
### 271 **3. Results**

#### 272 **3.1. Composition and antioxidant properties of Syrah red wines**

273 For this study, fourteen French Syrah red wines of 2019 vintage were collected directly from  
274 tanks and oak barrels in different winery of the Languedoc-Roussillon and Cotes du Rhône  
275 area. Before accelerated ageing tests, several parameters were measured on samples,  
276 including spectrophotometric measurements such as Folin-Ciocalteu total polyphenol content  
277 (TPC), total polyphenol index (TPI), total anthocyanins (TA) and absorbances at 420, 520 and  
278 620 nm for chromatic characteristics. Trolox equivalent antioxidant capacity (TEAC) by the  
279 ABTS assay, ferric reducing antioxidant power (FRAP) and cyclic voltammetry parameters  
280 (charges at various potentials) were measured in order to characterize the antioxidant  
281 capacity. Free sulfur dioxide determination was carried out by aeration/oxidation method.  
282 Analysis of monomeric anthocyanins and polymeric flavanols (after acid-catalyzed  
283 depolymerization) by UPLC-DAD-MS were also performed. Results are shown in  
284 Supplementary material (Table S1 - S5).

##### 285 **3.1.1. Syrah red wines composition**

286 In order to study the phenolic diversity and to identify possible groupings of the red wine  
 287 samples, a principal component analysis of the composition data was performed. Figure 1  
 288 shows the loadings and scores plots in the space described by the 1st and 2nd factors (total  
 289 explained variance of 48,42%). The first factor is mainly related to the richness in  
 290 anthocyanins (total and monomeric) and the second factor is positively correlated with the  
 291 composition in tannins.



292 *Figure 1. PCA analysis of composition data (wine samples and variables); 1: mDP; 2:*  
 293 *Epicatechin extension unit; 3: Catechin extension unit; 4: Acetylated anthocyanins; 5:*  
 294 *Coumaroylated anthocyanins; 6: Total monomeric anthocyanins; 7: Glycosylated*  
 295 *anthocyanins; 8: Free SO<sub>2</sub>; 9: Catechin terminal unit; 10: Total anthocyanins; 11: Total*  
 296 *flavanols; 12: TPC; 13: Epicatechin-3-O-gallate extension unit; 14: TPI; 15: Epicatechin*  
 297 *terminal unit; 16: Epigallocatechin extension unit; 17: % of galloylation; 18: Epicatechin-3-*

298 *O-gallate terminal unit; 19: % of prodelphinidin; 20: Epigallocatechin terminal unit (explained*  
299 *variance of 48,42%)*

300 The PCA showed that the samples were well distributed according to the composition  
301 variables. One sample seems to stand out from the others (LR1-C19), looking at the  
302 compositional data, this sample was characterised by a low concentration of anthocyanins  
303 (molecular and total) and a higher-than-average concentration of condensed tannins. Overall,  
304 the samples represented a good diversity, with no clustering by winery, origin, and type of  
305 ageing. This dataset and samples were then ideally adapted for applying PLS regression in  
306 order to construct models for predicting AATs.

### 307 **3.1.2. Correlation between physico-chemical parameters, antioxidants** 308 **capacity and the wine composition**

309 Table S6 (Supplementary Data) represented Pearson correlation coefficients ( $p(t) <$   
310  $0.05$  and  $p(t) < 0.01$ ) between wine composition (polyphenols and free  $\text{SO}_2$ ), antioxidant  
311 capacity (TEAC and FRAP), cyclic voltammetry charges and chromatic characteristics  
312 (absorbances). Concerning the phenolic composition, the TPC measured by Folin-Ciocalteu  
313 method, was not highly correlated as expected with TPI ( $R = 0.647$ ). This may be due to the  
314 fact that TPI is based on UV absorption while Folin-Ciocalteu is based on the reducing  
315 capacity of polyphenols. Besides, antioxidant capacity measured by colorimetric assays were  
316 well correlated with each other ( $R_{\text{TEAC/FRAP}} = 0.823$ ). In addition to that, total polyphenols  
317 (TPC and TPI) and colorimetric antioxidant assays (TEAC and FRAP) were correlated with  
318 all electrochemical parameters especially with  $Q_{240\text{mV}}$  and  $Q_{800\text{mV}}$  ( $R_{\text{TEAC}/Q_{240\text{mV}}} = 0.828$ ,  
319  $R_{\text{TPC}/Q_{240\text{mV}}} = 0.757$ ,  $R_{\text{FRAP}/Q_{240\text{mV}}} = 0.667$ ,  $R_{\text{TPI}/Q_{240\text{mV}}} = 0.626$   $R_{\text{TEAC}/Q_{800\text{mV}}} = 0.764$ ,  
320  $R_{\text{TPC}/Q_{800\text{mV}}} = 0.728$ ,  $R_{\text{FRAP}/Q_{800\text{mV}}} = 0.637$ ,  $R_{\text{TPI}/Q_{800\text{mV}}} = 0.728$ ) in accordance with previous  
321 studies (Benbouguerra et al., 2020; Deshaies et al., 2021; Newair et al., 2018). This could be  
322 explained by the fact that they are methods based on electron transfer from antioxidant to

323 oxidized compounds. Moreover, the different charge parameters measured by cyclic  
324 voltammetry were logically well correlated with each other ( $R_{Q_{800mV}/Q_{240mV}} = 0.822$ ,  
325  $R_{Q_{520mV}/Q_{240mV}} = 0.724$ ,  $R_{Q_{520mV}/Q_{520mV}-Q_{240mV}} = 0.949$ ). TPC was also strongly correlated with  
326 TEAC and FRAP assays respectively  $R = 0.83$  and  $R = 0.891$ . These results are in accordance  
327 with the literature as the different phenolic compounds present in the wines will be the  
328 predominant source of the antioxidant activity of red wines (Šeruga et al., 2011). TPC and  
329 FRAP assays were also correlated with total flavanols obtained after acidic depolymerization  
330 ( $R = 0.682$  and  $R = 0.698$ ) as shown previously (Newair et al., 2018). Correlations were found  
331 between spectrophotometric assays (TPC, FRAP and TEAC) and epigallocatechin extension  
332 unit. In addition, the electrochemical charges  $Q_{800mV}$  and  $Q_{240mV}$  are also correlated with these  
333 polymeric units,  $R = 0.783$  and  $R = 0.665$  respectively. This could be explained by the fact  
334 that the pyrogallol group (triphenol on the B-ring of the flavonoid) has a higher reducing  
335 power (Kilmartin & Hsu, 2003). The colour intensity was well correlated with the  
336 epicatechin-3-O-gallate extension units ( $R = 0.728$ ), which can be explained by the influence  
337 of the flavanol on the co-pigmentation reaction with anthocyanins leading to a hyperchromic  
338 effect (Boulton, 2001). At last, the composition in anthocyanins showed a positive correlation  
339 with free  $SO_2$  levels, in agreement with literature (Christofi et al., 2021).

## 340 **3.2. Comparison and PLS modelling of Accelerated Ageing Tests (AATs)**

### 341 **3.2.1. Comparison of Accelerated Ageing Tests**

342 Syrah red wine samples were subjected to three different accelerated ageing tests: chemical  
343 ( $H_2O_2$ -ATT), enzymatic (laccase-ATT) and thermal ( $60\text{ }^\circ\text{C}$ -ATT) (Deshaies et al., 2020) in  
344 order to study the influence of phenolic composition on the kinetic parameters of these AATs.  
345 After air saturation, initial dissolved oxygen levels were between 7 and 9 ppm. The evolution  
346 of oxygen consumption was monitored using fluorescence oxygen sensors. Oxygen  
347 consumption rate constant (k) for each AATs were calculated by exponential regression of

348 dissolved O<sub>2</sub> concentration as a function of time. As showed in Table S7 (Supplementary  
 349 Data) wine samples can differ in term of oxygen consumption kinetics parameters, these  
 350 results were in agreement with the literature (Deshaies et al., 2021; Ferreira et al., 2015).  
 351 Moreover, values differed between the tests and values ranged from 0.07 s<sup>-1</sup> to 1.81 s<sup>-1</sup> for  
 352 H<sub>2</sub>O<sub>2</sub>-AAT, from 0.05 s<sup>-1</sup> to 0.89 s<sup>-1</sup> for Laccase-AAT and at last from 0.15 s<sup>-1</sup> to 0.45 s<sup>-1</sup> for  
 353 60°C-AAT. Globally, chemical test using H<sub>2</sub>O<sub>2</sub> showed the highest oxygen consumption rate  
 354 constants for all considered samples except for, LR8-B19-2, CR12-B19-1 and CR12-B19-2,  
 355 for whom enzymatic test showed the highest consumption rate constants and thermal test for  
 356 LR8-B19-1. Concerning Pearson correlation (Table 2), no significant correlations (p = 0.05)  
 357 were found between the three different AATs.

358 *Table 2.* *Pearson's*  
 359 *correlation* *coefficients*  
 360 *between the*

	<b>H<sub>2</sub>O<sub>2</sub>-AAT</b>	<b>Laccase-AAT</b>	<b>60°C-AAT</b>
<b>H<sub>2</sub>O<sub>2</sub>-AAT</b>	<b>1</b>	0.010	0.523
<b>Laccase-AAT</b>	0.010	<b>1</b>	0.310
<b>60°C-AAT</b>	0.523	0.310	<b>1</b>

*three different*  
 361 *AATs*

362

363

364 These results suggest that different chemical mechanisms and targets are involved for each  
 365 AATs as the oxidising agents or temperature conditions that will accelerate or slow down  
 366 oxygen consumption. The concentration of these targets may therefore be a limiting factor in  
 367 the protection of the wine against oxidation and consequently in its ageing potential.

### 368 **3.2.2. Chemical Accelerated Ageing Tests: H<sub>2</sub>O<sub>2</sub>-AAT**

369 As the AATs showed different results depending on the test and the wine used, it appeared  
 370 necessary to investigate which parameters of the initial wine characteristics could impact  
 371 them. First, in order to investigate the individual influence of the wine different parameters

372 (phenolic, antioxidant and chromatic properties), a full linear correlation study was  
 373 performed. The list of parameters with significant Pearson correlation coefficients ( $p(t) <$   
 374  $0.05$ ) with the oxygen consumption constants for the  $H_2O_2$ -ATT ( $k_{H_2O_2}$ ) are shown in Table  
 375 3.A.

376 *Table 3: A. Pearson's correlation coefficients measured parameters and oxygen consumption*  
 377 *rate constant for the chemical AAT. \* represents significance at  $p \leq 0.01$  and # represents*  
 378 *significance at  $p \leq 0.05$ .*

379 *B. PLS regression coefficients and quality parameters for the different models explaining the*

A. $H_2O_2$ -AAT - Pearson correlation coefficients (# $p(t) < 0.05$ ; * $p(t) < 0.01$ )								
TPC	FRAP	TEAC	Epigallocatechin extension unit	Catechin terminal unit	Total flavanols	$Q_{800mV}$	$Q_{240mV}$	$Q_{520mV}$
0.654#	0.741*	0.654#	0.751*	0.622*	0.534*	0.631*	0.660*	0.574*
B. Modelling parameters		PCs	$r^2$	$H_2O_2$ -AAT - PLS Regression Model				
<b>Total</b>	4	0.928	TPC	Epigallocatechin extension unit	Catechin terminal unit	Epicatechin-3-O-gallate terminal unit	$A_{620}$	
			0.394	0.400	0.566	0.344	-0.382	
<b>Chemical composition</b>	3	0.920	Epigallocatechin extension unit	Catechin terminal unit	Epicatechin terminal unit	Epicatechin-3-O-gallate terminal unit	Total flavanols	
			0.689	0.641	-0.337	0.233	0.172	
<b>Antioxidant parameters</b>	3	0.621	FRAP	$Q_{240 mV}$	$Q_{520 mV}$			
			0.547	0.139	0.217			

380 *the  $H_2O_2$ -AAT results.*

381 Results of linear correlation revealed, that  $H_2O_2$ -AAT was positively correlated with the total  
 382 polyphenols content (TPC) and the total flavanols content measured after acidic  
 383 depolymerization. These results were in agreement with previous studies for wine model  
 384 solution (Danilewicz, 2007) and for real red wine (Ferreira et al., 2015) where the average  
 385 rate of oxygen consumption was related to total polyphenols. This highlights the antioxidant  
 386 character of total polyphenols. Moreover, the use of hydrogen peroxide, which is notably  
 387 involved in the Fenton reaction (A. L. Waterhouse & Laurie, 2006), will release a hydroxyl  
 388 radical  $\cdot OH$  that will accelerate the formation of the quinone of polyphenols and so oxygen

389 consumption is consequently increased. Noteworthy, a good positive correlation between the  
390 composition of epigallocatechin units and high H<sub>2</sub>O<sub>2</sub>-AAT was observed ( $R = 0.751$ ), which  
391 can be explained by the fact that prodelphinidins have an important antioxidant power  
392 (Ferreira et al., 2015; Kilmartin & Hsu, 2003). In addition to that, a positive correlation with  
393 the catechin terminal unit was also noted ( $R = 0.622$ ) was obtained. This positive influence of  
394 catechin on wine oxidation was in agreement with the literature (Márquez et al., 2019).  
395 Indeed, when hydrogen peroxide is added, the Fenton reaction is accelerated and accentuates  
396 the formation of acetaldehyde by oxidation of ethanol (Oliveira et al., 2011) which accelerates  
397 the oxygen consumption. The acetaldehyde thus formed will react with acetaldehyde-reactive-  
398 polyphenol (ARP) such as catechin to form ethyl-bridged polymers. Concerning the  
399 antioxidant parameters (TEAC, FRAP,  $Q_{800mV}$ ,  $Q_{240mV}$  and  $Q_{520mV}$ ), as shown in section 3.1.b,  
400 these parameters were correlated with the polyphenol composition. It is therefore logical that  
401 they were also correlated with the H<sub>2</sub>O<sub>2</sub>-AAT values.

402 As the linear correlation study showed, the H<sub>2</sub>O<sub>2</sub>-AAT values were only weakly correlated  
403 with the individual parameters of the chemical composition or the antioxidant properties of  
404 the wine. This confirmed that the H<sub>2</sub>O<sub>2</sub>-AAT values were influenced by multiple factors and  
405 PLS models provided better results with satisfactory predictive power. The results of the most  
406 relevant variables and their normalized coefficients in the regression equation were  
407 summarised in Table 3.B. Three different PLS regression models were established  
408 considering: all the measured parameters (1), only the composition variables (2) and at last  
409 only the antioxidant parameters (3). PLS models (1) and (2) showed a good correlation  
410 between the predicted and experimental values of the H<sub>2</sub>O<sub>2</sub>-AAT values with a linearity  
411 coefficient ( $r^2$ ) of 0.928 and 0.920 respectively (Figure S1, Supplementary Data). However,  
412 for the model (3) which take only the antioxidant parameters into account, the model did not  
413 give a high linearity ( $r^2 = 0.621$ ) which means that the oxidation mechanisms of the H<sub>2</sub>O<sub>2</sub>-

414 AAT were less related to these parameters. In addition to that, some variables were only  
415 relevant for the multivariate model (Table 2.B.) and it was not possible to establish a linear  
416 correlation for them with the H<sub>2</sub>O<sub>2</sub>-AAT results. These variables included epicatechin-3-O-  
417 gallate terminal unit and A<sub>620</sub> for model (1) and epicatechin terminal unit and epicatechin-3-  
418 O-gallate terminal unit for model (2). This means that there was no direct relationship of the  
419 concentration of these parameters on oxygen consumption, but the interactions between these  
420 compounds were important in the oxidative process.

421 PLS models (1) and (2) suggested that red wine rich in the terminal epicatechin-3-O-gallate  
422 unit had faster chemical oxidation kinetics and thus higher H<sub>2</sub>O<sub>2</sub>-AAT values. This result is in  
423 agreement with previous study (Carrascón et al., 2018) which showed that epicatechin-3-O-  
424 gallate units were rapidly consumed in wines with high oxygen consumption rates. This result  
425 highlights the reducing properties of this flavan-3-ol through the presence of a trihydroxyl  
426 group in the galloyl moiety that may be important in radical scavenging. Additionally, model  
427 (2) indicated that the epicatechin end unit was negatively related to the H<sub>2</sub>O<sub>2</sub>-AAT values.  
428 This result could be surprising but previous studies (Carrascón et al., 2018; Ferreira et al.,  
429 2015; Márquez et al., 2019) showed the negative role of epicatechin polymeric units on  
430 oxygen consumption and wine oxidation. A possible explanation for this result could be the  
431 possible formation of chelation complexes between the hydroxyl functions of the polyphenols  
432 and some metal ions (iron and copper) which may disrupt the catalytic oxidation cycle  
433 (Perron & Brumaghim, 2009). At last, it was observed in the model (1) that the negative  
434 contribution of the absorbance at 620 nm corresponding to the absorbance of polymeric  
435 pigments whose maximum absorption wavelength induces a blue-violet tone through  
436 hyperchromic shift (Boulton, 2001). This result could be explained by the fact that polymeric  
437 pigments have a higher resistance to oxidation than native pigments, thus resulting in a lower  
438 oxygen consumption rate and lower H<sub>2</sub>O<sub>2</sub>-AAT values.

### 3.2.3. Enzymatic Accelerated Ageing Test: laccase-ATT

440 For the Laccase-AAT, the oxidation of the sample is catalysed by laccases which are  
 441 polyphenoloxidase (PPO) enzymes derived from fungi. The laccases use molecular oxygen to  
 442 oxidise polyphenols through free radical reaction mechanism. Polyphenols are oxidation  
 443 substrates for these enzymes which can have two types of activity, monophenol oxidase  
 444 activity characterised by the hydroxylation of a monophenol to a diphenol and diphenol  
 445 oxidase activity corresponding to the oxidation of dihydroxybenzenes to benzoquinones  
 446 (Oliveira et al., 2011).

447 In order to investigate the parameters influencing the oxygen consumption kinetics of laccase-  
 448 AAT, a chemometric analysis similar to the chemical test was performed. First, a full linear  
 449 correlation study was performed and the list of parameters showing significant Pearson  
 450 correlation coefficients ( $p(t) < 0.05$ ) with the oxygen consumption constants for laccase-AAT  
 451 ( $k_{\text{laccase}}$ ) are compiled in Table 4.A.

452 *Table 4: A. Pearson's correlation coefficients measured parameters and oxygen consumption*  
 453 *rate constant for the Laccase-AAT. \* represents significance at  $p \leq 0.01$  and # represents*  
 454 *significance at  $p \leq 0.05$ .*

455 *B. PLS regression coefficients and quality parameters for the different models explaining the*  
 456 *oxygen consumption rate constant for the Laccase-AAT.*

A.		Laccase-AAT - Pearson correlation coefficients (# $p(t) < 0.05$ ; * $p(t) < 0.01$ )							
Catechin extension unit	mDP								
0.638#	0.750*								
B. Modelling parameters		PCs	$r^2$	Laccase-AAT - PLS Regression Model					
	Total	4	0.956	TPI	Acetylated anthocyanins	Epicatechin extension unit	Epicatechin-3-O-gallate extension unit	Free SO <sub>2</sub>	A <sub>620</sub>
				0.319	0.877	0.382	-0.542	-0.901	0.412
	Chemical composition	4	0.980	TPI	TA	Catechin extension unit	Epicatechin extension unit	Epicatechin-3-O-gallate extension unit	Free SO <sub>2</sub>

			0.271	0.706	0.452	0.367	-0.579	-0.742
<b>Antioxidant parameters</b>	4	0.186	FRAP	Q <sub>800mV</sub>	Q <sub>240 mV</sub>	Q <sub>240mV</sub> / Q <sub>800mV</sub>		
			0.320	5.591	-6.797	3.744		

457

458 The results of the linear correlation revealed that Laccase-AAT was positively correlated with  
459 only two variables, the catechin extension unit and the mean degree of polymerization (mDP).  
460 Concerning the catechin extension units of tannins were correlated ( $R = 0.638$ ), it has been  
461 reported in the literature that polyphenols of the 1-2 dihydroxybenzene type such as catechol  
462 or galloyl groups are preferential substrates for oxidation by laccases (Deshaies et al., 2020;  
463 Oliveira et al., 2011). An unexpected and outstanding result is that Laccase-AAT is positively  
464 correlated with the mDP ( $R = 0.750$ ). Indeed, steric hindrance plays an important role during  
465 oxidation reactions by laccases, the reactivity of laccases towards different substrates is all the  
466 weaker as the substituents are voluminous (Nicolas et al., 2003). It seems that oxygen  
467 consumption during enzymatic oxidation was impacted by the size of the condensed tannins.  
468 However, the mDP values (table S8, Supplementary Data) were low and the range of the  
469 values limited (min = 1.94 and max = 3.79), so there was not an important variation of this  
470 parameter between the samples.

471 Overall, the linear correlation study showed that Laccase-AAT results are poorly correlated  
472 with the measured wine initial parameters. This accelerated ageing test is then probably  
473 dependent on multiple factors. This hypothesis was confirmed by the establishment of three  
474 PLS regression models with good predictive values.

475 Models (1) and (2) showed high correlations between the predicted and experimental values  
476 of Laccase-AAT with a linearity coefficient ( $r^2$ ) of 0.956 and 0.980 respectively (Figure S2,  
477 Supplementary Data). But model (3) showed no linearity ( $r^2 = 0.186$ ) which means that the  
478 antioxidant parameters alone are not able to predict this enzymatic test. The results of the

479 most relevant variables and their standardised coefficients in the regression equation are  
480 summarised in Table 4.B.

481 PLS Models (1) and (2) suggested that red wine with high total polyphenol index (TPI) had  
482 faster enzymatic oxidation kinetics ( $k_{\text{laccase}}$ ) during the laccase-AAT test. This TPI index  
483 provided an estimation of the total phenolic compounds with a benzene ring. This result was  
484 in agreement with the literature (Deshaies et al., 2020; Oliveira et al., 2011; A. Waterhouse et  
485 al., 2016) where it was showed that polyphenols, in particular flavan-3-ols, were the main  
486 substrates for laccase oxidation. This result corroborated the positive influence of epicatechin  
487 extension units (model (1)) and catechin extension units (model (2)) on this accelerated  
488 enzymatic ageing test. In addition, catechin was the variable that contributes the most to the  
489 Laccase-AAT as it was both linearly correlated and relevant to the multivariate model (2).  
490 The epicatechin-3-O-gallate extension units were found to contribute negatively to both  
491 models (1) and (2). It would therefore appear that red wines with high concentrations of this  
492 polymeric unit would have lower Laccase-AAT values. Moreover, it was also reported  
493 (Cheynier & Ricardo da Silva, 1991) that galloylated procyanidins were not the main targets  
494 of oxidation reactions by polyphenol oxidase (PPO). Furthermore, the negative influence of  
495 the free SO<sub>2</sub> content on model (1) and (2) can be noted. This result was consistent with the  
496 literature (Toit et al., 2006) where it has been shown that higher SO<sub>2</sub> concentration lower the  
497 laccase activity.

498 It was also observed that the concentration of acetylated anthocyanins had a positive impact  
499 on PLS model (1) and total anthocyanins (TA) on PLS model (2). At first sight, anthocyanins  
500 were not the main substrates for laccase oxidation and this limited activity was probably  
501 related to the presence of a glycosidic moiety that would cause steric hindrance. However,  
502 these compounds, although not direct substrates of the enzyme, can actively participate in  
503 browning by coupled oxidation reactions. The degradation of anthocyanins was strongly

504 accelerated in the presence of caffeic acid derivatives or catechins (Sarni-Manchado et al.,  
 505 1997). As shown previously (Deshaies et al., 2020), during this accelerated test, a decrease in  
 506 the anthocyanin ion intensity using LC-HMRS analysis occurred. Additionally, the PLS  
 507 model (1) indicated that the Laccase-AAT was positively related to the absorbance at 620 nm.

### 508 3.2.4. Thermal Accelerated Ageing Test: 60°-ATT

509 For the thermal 60°-ATT, the increase in temperature accelerated and catalysed all  
 510 endothermic reactions such as many oxidation reactions. Another chemometric analysis of the  
 511 60°-ATT was performed. A full linear correlation study was first obtained and the list of  
 512 parameters showing significant Pearson correlation coefficients ( $p(t) < 0.05$ ) with the oxygen  
 513 consumption constants for 60°-ATT was compiled in Table 5.A.

514 *Table 5: A. Pearson's correlation coefficients measured parameters and oxygen consumption*  
 515 *rate constant for the 60°-ATT. \* represents significance at  $p \leq 0.01$  and # represents*  
 516 *significance at  $p \leq 0.05$ .*

517 *B. PLS regression coefficients and quality parameters for the different models explaining the*  
 518 *oxygen consumption rate constant for the 60°-ATT.*

A									
60°-ATT - Pearson correlation coefficients (# $p(t) < 0.05$ ; * $p(t) < 0.01$ )									
FRAP	Glycosylated anthocyanins	Acetylated anthocyanins	Coumaroylated anthocyanins	Total monomeric anthocyanins	Catechin extension unit	Catechin terminal unit	$Q_{520mV}$	$Q_{520mV} - Q_{240mV}$	
0.614#	0.536#	0.598#	0.688*	0.578#	0.637#	0.627#	0.585#	0.590#	
B									
Modelling parameters	PCs	$r^2$	60°-ATT - PLS Regression Model						
Total	4	0.967	FRAP	Acetylated anthocyanins	Catechin extension unit	Catechin terminal unit	$Q_{240 mV}$	$Q_{520mV} - Q_{240mV}$	
			0.267	0.426	0.207	0.386	-0.260	0.450	
Chemical composition	4	0.892	Acetylated anthocyanins	Total monomeric anthocyanins	Epigallocatechin terminal unit	Catechin terminal unit	Epicatechin extension unit	Free SO <sub>2</sub>	
			0.495	0.341	-0.379	0.439	0.161	-0.370	
Antioxidant parameters	4	0.748	FRAP	ABTS	$Q_{240mV} / Q_{800mV}$	$Q_{520mV} - Q_{240mV}$			
			1.083	-0.790	0.173	0.483			

519 Results of linear correlation revealed that 60°-ATT was only positively correlated with many  
 520 parameters contrary to the two other tests. Outstandingly, it should be noted that all  
 521 monomeric anthocyanins (glycolysed, acetylated, coumaroylated, total monomeric) measured

522 by UHPLC were positively correlated with the 60°-ATT. Due to the increase in temperature  
523 (60°C), many reactions are catalysed and in particular the formation of highly reactive  
524 quinones (Deshaies et al., 2020), which by metallic catalysis via the Fenton reaction will lead  
525 to the formation of hydroxyl radicals, hydrogen peroxide and acetaldehyde (Oliveira et al.,  
526 2011; A. L. Waterhouse & Laurie, 2006) and thus accelerate oxygen consumption. The  
527 acetaldehyde formed can react with acetaldehyde-reactive polyphenols (ARP) such as  
528 monomeric anthocyanins to form new polymerised pigments with flavanols (Echave et al.,  
529 2021) and can lead to the formation of new anthocyanin-derived pigments such as  
530 pyranoanthocyanins (Carrascón et al., 2018; Fulcrand et al., 1998). Moreover, anthocyanins  
531 are also thermolabile compounds and chemical modifications such as deglycosylation when  
532 the temperature is increased may occur. These different temperature-catalysed reactions  
533 therefore increased the consumption of oxygen during the 60°-ATT.

534 In addition to that, a positive correlation with the catechin polymeric unit (extension and  
535 terminal unit) was obtained ( $R = 0.637$  and  $R = 0.627$  respectively) and was consistent with  
536 the results of the  $H_2O_2$ -ATT. Indeed, when the temperature increased, the formation of  
537 quinone by the Fenton reaction was accelerated and accentuated the formation of  
538 acetaldehyde by oxidation of ethanol. The antioxidant capacity measured by the FRAP assay  
539 was also positively correlated with 60°-ATT. Due to the fact that a wine with a high reducing  
540 capacity have a better ability to resist to oxidation (Singleton, 1987) through its phenolic pool,  
541 therefore a wine with a high antioxidant capacity will consume oxygen more quickly.

542 Two electrochemical parameters were correlated with 60°-ATT. The charge at 520 mV  
543 ( $Q_{520mV}$ ) which corresponds to all the compounds that oxidise up to this potential such as  
544 catechin-type flavanols, malvidin-based anthocyanins and galloylated compounds. While the  
545 difference of charges  $Q_{520mV} - Q_{240mV}$  which corresponds only to the charge resulting from  
546 oxidation of malvidin-based anthocyanins and the second oxidation of ortho-diphenols such

547 as catechin (Benbouguerra et al., 2020; Deshaies et al., 2021; Newair et al., 2018). Positive  
548 correlations between 60°-ATT and anthocyanins and catechin-based polymeric units were  
549 also obtained. These compounds, which correspond to the electrochemical charge  $Q_{520mV}$  and  
550 the difference of charges  $Q_{520mV}-Q_{240mV}$ , consequently explain these positive correlations.

551 As for the other two tests, the Pearson coefficients obtained did not allow us to establish clear  
552 correlations when individual parameters were used. Three PLS regression models were  
553 therefore built as for the  $H_2O_2$ -ATT and laccase-AAT. PLS modelling allowed to find highly  
554 significant models linking the 60°-ATT values to the initial wine measured parameters. PLS-  
555 Model (1) considering both compositional and antioxidant parameters showed the best  
556 correlation between the predicted and experimental values of 60°-ATT with a linearity  
557 coefficient ( $r^2$ ) of 0.967. Model (2) taking into account only the compositional parameters  
558 showed a lower correlation than model (1) with an  $r^2$  of 0.892. Finally, contrary to the to the  
559  $H_2O_2$ -ATT and laccase-AAT, PLS-model (3) (antioxidant parameters) showed a linearity with  
560 the antioxidant parameters with the lowest obtained correlation coefficient ( $r^2$ ) of 0.748  
561 (Figure S3, Supplementary Data). These results showed that it was necessary to consider all  
562 the measured parameters to predict this thermal test. The results of the most relevant variables  
563 for each PLS regression and their standardised coefficients in the regression equation have  
564 been summarised in Table 5.B. There were variables that were only relevant for the  
565 multivariate model, but for which it was not possible to establish a linear correlation with the  
566 60°C-ATT.

567 Concerning the PLS-model (1), among the most important parameters, some were both  
568 linearly positively correlated and relevant for the multivariate model, indicating a direct effect  
569 of these compounds on this AAT result. The model suggested a positive influence of  
570 antioxidant capacity measured by FRAP assay, acetylated anthocyanins, extension and  
571 terminal catechin units, and the difference of electrochemical charge  $Q_{520mV}-Q_{240mV}$ . AS

572 explained previously, these parameters were positively related to the oxygen consumption  
573 during thermal AAT through the acceleration of oxidation reactions caused by the increase in  
574 temperature (Deshaies et al., 2020). Unfortunately, PLS model (1) showed that the  
575 electrochemical charge at 240 mV ( $Q_{240mV}$ ) which represents the most easily oxidisable  
576 polyphenols groups such as pyrogallol group (Kilmartin & Hsu, 2003) impacted negatively  
577 this regression model. In addition to that, PLS-model (2) also showed negative impact of the  
578 epigallocatechin terminal unit. However, some studies showed that certain polyphenols could  
579 have a negative influence on oxygen consumption (Carrascón et al., 2018; Ferreira et al.,  
580 2015). It has also been shown (Jovanovic et al., 1998) that epigallocatechin type flavanols  
581 could form relatively stable complexes with metal ions that at pH of wine. These complexes  
582 could therefore slow down the Fenton reaction by decreasing the concentration of free metal  
583 ions. However, the opposite behaviour was obtained for the model (1) and (2) of the chemical  
584 AAT, which could be explained by the addition of hydrogen peroxide in excess which  
585 promoted the formation of an ethoxyl radical (Deshaies et al., 2020) which oxidised the wine  
586 polyphenols more quickly.

587 Furthermore, according to model (2), the kinetic parameters of the thermal test were  
588 positively influenced by the epicatechin extension units. Like catechin, this flavan-3-ol was  
589 also substrate for non-enzymatic oxidation by the Fenton reaction (Oliveira et al., 2011).  
590 Conversely, the free  $SO_2$  content has a negative influence on the thermal ATT constant. This  
591 may seem surprising as  $SO_2$  being an antioxidant should accelerate oxygen consumption  
592 (Danilewicz, 2007) but Carrascón et al. (Carrascón et al., 2018) showed that there was no  
593 influence of  $SO_2$  on the oxygen consumption of red wine. However, in our study, oxygen  
594 consumption was monitored during accelerated ageing and when the temperature was  
595 increased in acidic media like wine matrix, many chemical reactions were accelerated, in  
596 particular reactions related to tannins, as depolymerisation reactions. These depolymerised

597 tannins may then react with SO<sub>2</sub> to give flavanol sulfonate (Bonaldo et al., 2020). These  
598 reactions could therefore make SO<sub>2</sub> less available to react with oxygen.

#### 599 **4. Conclusion**

600 In this work, three accelerated ageing tests (60°C-ATT, Laccase-ATT and H<sub>2</sub>O<sub>2</sub>-ATT) were  
601 applied to Syrah red wines with different phenolic compositions and antioxidant properties  
602 showing that the results of the tests were not correlated with each other. These results  
603 therefore revealed specific mechanisms for each accelerated ageing test. This was  
604 corroborated by linear correlations and multivariate PLS models between the measured  
605 variables and the accelerated tests that differed for each test.

606 Results also illustrated that some chemical and antioxidant parameters were useful variables  
607 to predict the results of three different accelerated ageing tests. Although some individual  
608 variables were linearly correlated with the AATs results, PLS models, using a multi-variable  
609 approach, were much more precise and powerful to predict them.

610 These different accelerated ageing tests could be complementary for each other to predict red  
611 wine ageing. In future work, other measurements involving wine samples undergoing  
612 “natural” ageing were done to determine if one or more than one AAT(s) are needed to  
613 predict red wine ageing kinetics.

#### 614 **Funding**

615 This work was supported in part by a research contract between Diam Bouchage and the  
616 University of Montpellier (200893).

617

618

619

620

621 **References**

- 622 Alcalde-Eon, C., Escribano-Bailón, M. T., Santos-Buelga, C., & Rivas-Gonzalo, J. C. (2006).  
623 Changes in the detailed pigment composition of red wine during maturity and ageing :  
624 A comprehensive study. *Analytica Chimica Acta*, 563(1), 238-254.  
625 <https://doi.org/10.1016/j.aca.2005.11.028>
- 626 Benbouguerra, N., Richard, T., Saucier, C., & Garcia, F. (2020). Voltammetric Behavior,  
627 Flavanol and Anthocyanin Contents, and Antioxidant Capacity of Grape Skins and  
628 Seeds during Ripening (*Vitis vinifera* var. Merlot, Tannat, and Syrah). *Antioxidants*,  
629 9(9), 800. <https://doi.org/10.3390/antiox9090800>
- 630 Bonaldo, F., Guella, G., Mattivi, F., Catorci, D., & Arapitsas, P. (2020). Kinetic investigations  
631 of sulfite addition to flavanols. *Scientific Reports*, 10(1), Art. 1.  
632 <https://doi.org/10.1038/s41598-020-69483-0>
- 633 Boulton, R. (2001). The Copigmentation of Anthocyanins and Its Role in the Color of Red  
634 Wine : A Critical Review. *American Journal of Enology and Viticulture*, 52(2), 67-87.
- 635 Brouillard, R., George, F., & Fougerousse, A. (1997). Polyphenols produced during red wine  
636 ageing. *BioFactors*, 6(4), 403-410. <https://doi.org/10.1002/biof.5520060406>
- 637 Carrascón, V., Vallverdú-Queralt, A., Meudec, E., Sommerer, N., Fernandez-Zurbano, P., &  
638 Ferreira, V. (2018). The kinetics of oxygen and SO<sub>2</sub> consumption by red wines. What  
639 do they tell about oxidation mechanisms and about changes in wine composition?  
640 *Food Chemistry*, 241, 206-214. <https://doi.org/10.1016/j.foodchem.2017.08.090>
- 641 Cheynier, V., & Ricardo da Silva, J. M. (1991). Oxidation of grape procyanidins in model  
642 solutions containing trans-caffeoyltartaric acid and polyphenol oxidase. *Journal of*  
643 *Agricultural and Food Chemistry*, 39(6), 1047-1049.  
644 <https://doi.org/10.1021/jf00006a008>

645 Christofi, S., Katsaros, G., Mallouchos, A., Cotea, V., & Kallithraka, S. (2021). Reducing SO<sub>2</sub>  
646 content in wine by combining High Pressure and glutathione addition. *OENO One*,  
647 55(1), Art. 1. <https://doi.org/10.20870/oeno-one.2021.55.1.4558>

648 Danilewicz, J. C. (2007). Interaction of Sulfur Dioxide, Polyphenols, and Oxygen in a Wine-  
649 Model System : Central Role of Iron and Copper. *American Journal of Enology and*  
650 *Viticulture*, 58(1), 53-60.

651 Deshaies, S., Cazals, G., Enjalbal, C., Constantin, T., Garcia, F., Mouls, L., & Saucier, C.  
652 (2020). Red Wine Oxidation : Accelerated Ageing Tests, Possible Reaction  
653 Mechanisms and Application to Syrah Red Wines. *Antioxidants*, 9(8), Art. 8.  
654 <https://doi.org/10.3390/antiox9080663>

655 Deshaies, S., Garcia, L., Veran, F., Mouls, L., Saucier, C., & Garcia, F. (2021). Red Wine  
656 Oxidation Characterization by Accelerated Ageing Tests and Cyclic Voltammetry.  
657 *Antioxidants (Basel, Switzerland)*, 10(12), 1943.  
658 <https://doi.org/10.3390/antiox10121943>

659 Echave, J., Barral, M., Fraga-Corral, M., Prieto, M. A., & Simal-Gandara, J. (2021). Bottle  
660 Aging and Storage of Wines : A Review. *Molecules*, 26(3), Art. 3.  
661 <https://doi.org/10.3390/molecules26030713>

662 Ferreira, V., Bueno, M., Franco-Luesma, E., Culleré, L., & Fernández-Zurbano, P. (2014).  
663 Key Changes in Wine Aroma Active Compounds during Bottle Storage of Spanish  
664 Red Wines under Different Oxygen Levels. *Journal of Agricultural and Food*  
665 *Chemistry*, 62(41), 10015-10027. <https://doi.org/10.1021/jf503089u>

666 Ferreira, V., Carrascon, V., Bueno, M., Ugliano, M., & Fernandez-Zurbano, P. (2015).  
667 Oxygen Consumption by Red Wines. Part I : Consumption Rates, Relationship with  
668 Chemical Composition, and Role of SO<sub>2</sub>. *Journal of Agricultural and Food*  
669 *Chemistry*, 63(51), 10928-10937. <https://doi.org/10.1021/acs.jafc.5b02988>

670 Fulcrand, H., Benabdeljalil, C., Rigaud, J., Cheynier, V., & Moutounet, M. (1998). A new  
671 class of wine pigments generated by reaction between pyruvic acid and grape  
672 anthocyanins. *Phytochemistry*, 47(7), 1401-1407. <https://doi.org/10.1016/S0031->  
673 9422(97)00772-3

674 Gambuti, A., Rinaldi, A., Ugliano, M., & Moio, L. (2013). Evolution of Phenolic Compounds  
675 and Astringency during Aging of Red Wine : Effect of Oxygen Exposure before and  
676 after Bottling. *Journal of Agricultural and Food Chemistry*, 61(8), 1618-1627.  
677 <https://doi.org/10.1021/jf302822b>

678 Jovanovic, S. V., Simic, M. G., Steenken, S., & Hara, Y. (1998). Iron complexes of  
679 galliccatechins. Antioxidant action or iron regulation? *Journal of the Chemical Society,*  
680 *Perkin Transactions 2*, 0(11), 2365-2370. <https://doi.org/10.1039/A805894F>

681 Kilmartin, P. A. (2009). The Oxidation of Red and White Wines and its Impact on Wine  
682 Aroma. *Chemistry in NZ*, 5.

683 Kilmartin, P. A., & Hsu, C. F. (2003). Characterisation of polyphenols in green, oolong, and  
684 black teas, and in coffee, using cyclic voltammetry. *Food Chemistry*, 82(4), 501-512.  
685 [https://doi.org/10.1016/S0308-8146\(03\)00066-9](https://doi.org/10.1016/S0308-8146(03)00066-9)

686 Márquez, K., Pérez-Navarro, J., Hermosín-Gutiérrez, I., Gómez-Alonso, S., Mena-Morales,  
687 A., García-Romero, E., & Contreras, D. (2019). Systematic study of hydroxyl radical  
688 production in white wines as a function of chemical composition. *Food Chemistry*,  
689 288, 377-385. <https://doi.org/10.1016/j.foodchem.2019.03.005>

690 Muller, L., Gnoyke, S., Popken, A. M., & BOhm, V. (2010). Antioxidant capacity and related  
691 parameters of different fruit formulations. *Food Science and Technology*, 8.

692 Newair, E. F., Kilmartin, P. A., & Garcia, F. (2018). Square wave voltammetric analysis of  
693 polyphenol content and antioxidant capacity of red wines using glassy carbon and  
694 disposable carbon nanotubes modified screen-printed electrodes. *European Food*

695           *Research and Technology*, 244(7), 1225-1237. <https://doi.org/10.1007/s00217-018->  
696           3038-z

697 Nicolas, J., Billaud, C., Phlippon, J., & Rouet-Mayer, A.-M. (2003). Enzymatic browning –  
698           Biochemical Aspects. In *Encyclopedia of food sciences and nutrition* (2nd éd., p.  
699           678-686). Oxford Academic Press.

700 Oliveira, C. M., Ferreira, A. C. S., De Freitas, V., & Silva, A. M. S. (2011). Oxidation  
701           mechanisms occurring in wines. *Food Research International*, 44(5), 1115-1126.  
702           <https://doi.org/10.1016/j.foodres.2011.03.050>

703 Perron, N. R., & Brumaghim, J. L. (2009). A Review of the Antioxidant Mechanisms of  
704           Polyphenol Compounds Related to Iron Binding. *Cell Biochemistry and Biophysics*,  
705           53(2), 75-100. <https://doi.org/10.1007/s12013-009-9043-x>

706 Ribéreau-Gayon, P. (1970). Les dosages des composés phénoliques totaux dans les vins  
707           rouges. *Chim. Anal*, 52, 627-631.

708 Ribéreau-Gayon, P., & Peynaud, E. (1966). *Traité d'oenologie : Composition,*  
709           *Transformations et Traitements des vins*. LIBRAIRIE POLYTECHNIQUE CH  
710           BERANGER.

711 Ribéreau-Gayon, P., & Stonestreet, E. (1965). Le dosage des anthocyanes dans le vin rouge.  
712           *Bulletin de la Société chimique de France*, 9, 2649-2652.

713 Salas, E., Atanasova, V., Poncet-Legrand, C., Meudec, E., Mazauric, J. P., & Cheynier, V.  
714           (2004). Demonstration of the occurrence of flavanol–anthocyanin adducts in wine and  
715           in model solutions. *Analytica Chimica Acta*, 513(1), 325-332.  
716           <https://doi.org/10.1016/j.aca.2003.11.084>

717 Sarni-Manchado, P., Cheynier, V., & Moutounet, M. (1997). Reactions of polyphenoloxidase  
718           generated caftaric acid o-quinone with malvidin 3-O-glucoside. *Phytochemistry*, 45(7),  
719           1365-1369. [https://doi.org/10.1016/S0031-9422\(97\)00190-8](https://doi.org/10.1016/S0031-9422(97)00190-8)

720 Šeruga, M., Novak, I., & Jakobek, L. (2011). Determination of polyphenols content and  
721 antioxidant activity of some red wines by differential pulse voltammetry, HPLC and  
722 spectrophotometric methods. *Food Chemistry*, 124(3), 1208-1216.  
723 <https://doi.org/10.1016/j.foodchem.2010.07.047>

724 Singleton, V. L. (1987). Oxygen with Phenols and Related Reactions in Musts, Wines, and  
725 Model Systems : Observations and Practical Implications. *American Journal of*  
726 *Enology and Viticulture*, 38(1), 69-77.

727 Suleria, H. A. R., Barrow, C. J., & Dunshea, F. R. (2020). Screening and Characterization of  
728 Phenolic Compounds and Their Antioxidant Capacity in Different Fruit Peels. *Foods*,  
729 9(9), Art. 9. <https://doi.org/10.3390/foods9091206>

730 Tao, Y., García, J. F., & Sun, D.-W. (2014). Advances in Wine Aging Technologies for  
731 Enhancing Wine Quality and Accelerating Wine Aging Process. *Critical Reviews in*  
732 *Food Science and Nutrition*, 54(6), 817-835.  
733 <https://doi.org/10.1080/10408398.2011.609949>

734 Toit, W. J. du, Marais, J., Pretorius, I. S., & Toit, M. du. (2006). Oxygen in Must and Wine :  
735 A review. *South African Journal of Enology and Viticulture*, 27(1), Art. 1.  
736 <https://doi.org/10.21548/27-1-1610>

737 Ugliano, M. (2013). Oxygen Contribution to Wine Aroma Evolution during Bottle Aging.  
738 *Journal of Agricultural and Food Chemistry*, 61(26), 6125-6136.  
739 <https://doi.org/10.1021/jf400810v>

740 Vivas, N., & Glories, Y. (1996). Role of Oak Wood Ellagitannins in the Oxidation Process of  
741 Red Wines During Aging. *American Journal of Enology and Viticulture*, 47(1),  
742 103-107.

743 Waterhouse, A. L., & Laurie, V. F. (2006). Oxidation of Wine Phenolics : A Critical  
744 Evaluation and Hypotheses. *American Journal of Enology and Viticulture*, 57(3),  
745 306-313.

746 Waterhouse, A. L., & Miao, Y. (2021). Can Chemical Analysis Predict Wine Aging  
747 Capacity? *Foods*, 10(3), Art. 3. <https://doi.org/10.3390/foods10030654>

748 Waterhouse, A., Sacks, G., & Jeffery, D. (2016). *Understanding Wine Chemistry* (Wiley).

749

750

751

752

753

754

755

756

757

758